3.2.1. EFFECTS OF VARIABLE MICROACCELERATIONS IN DISTRIBUTION OF IMPURITY INHOMOGENEITIES IN THE InSb:Te SINGLE CRYSTALS GROWN BY CRUCIBLELESS FLOATING ZONE MELTING ON THE "FOTON" SATELLITE

The contemporary data on low-frequency micro-accelerations, that are typical for all satellites of a "Foton" series, are compared with the peculiarities of impurity inhomogeneity distributions revealed in Te-doped indium antimonide single crystal (InSb:Te), grown by floating zone melting technique during the "Foton-3" flight mission. Within a complicated structure of these inhomogeneities (as a shape and position of the impurity core as the striations) a lot of periodicity is occurred. The frequencies of this periodicity are detected by a method of spectral image analysis of the numeric coding photos of a central longitudinal section of the investigated crystal. These frequencies coincide with those detected in micro-accelerations in a range of 0-0.005 Hz measured on the recent "Fotons". It testifies that the reasons of origin of indicated periodicity were quasi-stationary micro-accelerations onboard the satellite, and confirms developed representations how the small forces of gravity and inertial nature influence convective heat/mass transfer in melts and, as a result, the segregation processes during crystal growth by directional crystallization methods.

Introduction

In our papers [1–9] was already communicated about the studies of the impurity inhomogeneities in the Te-doped single crystals of indium antimonide (InSb:Te), which for the first time were grown in microgravity by the floating zone melting (FZM) technique onboard the "Foton-3" satellite. In the longitudinal sections of these single crystals an unusually complicated, quasi-periodic structures of impurity inhomogeneities such as an impurity core (a facet effect) [1-7], and the striations [8, 9] were detected. These phenomena can be explained within the framework of physical representations developed in [4-9] and mathematical numerical simulation [10, 11]. According to these representations, the variable on magnitude and direction quasi-stationary (with the frequencies $f < 0.01$ Hz) micro-accelerations (μg), operating onboard space vehicles, are responsible for an origin of inhomogeneities of impurities distribution in the crystals, grown in microgravity by directional crystallization. These μg, i.e. the small forces of gravity and inertial nature, influence the fields of flow, temperature and concentration in the melts and, as a result, the segregation and arising of impurity inhomogeneities in the single crystals, growing from the melts [12].

For FZM the possibility of such effects under μg action is confirmed by numerical solution of 2D-problems accounting convection of buoyancy and capillary types in a melt with constant μg directed along or across liquid zone [5], and with μg, periodically varying on magnitude and operating along a centerline of the growing crystal [13].

To get experimental data, using which it is possible to prove a connection of peculiarities of a structure of inhomogeneities in the crystals with μg-changes, until now was hampered by absence of regular μg-measurements (especially in a frequency range $f < 0.01$ Hz) during majority experiments carried out onboard spacecraft, including "Foton-3". On the satellites of a "Foton" series such

measurements started since 1992 (“Foton-8” - “Foton-10” [14, 15]) and actively were carried out on “Foton-11” and “Foton-12” [16, 17]. In [18–21] a detail mathematical treatment and analysis of μg data, obtained by various methods on “Foton-11” and “Foton-12”, are made, and a spectrum of low-frequency μg, being characteristic for the spacecraft of a “Foton” series, is established. Due to these results, a possibility for the first time has appeared to compare periodicity in a structure of the impurity core and striations detected in the InSb:Te single crystal, grown by FZM in the “Foton-3” flight, with the frequencies of μg, operating onboard space vehicles of this type.

Methodology of FZM experiments

The InSb:Te FZM experiments were carried out using the “Zona-4” furnace onboard the “Foton-3” [1, 2]. The initial single crystalline ingots with a diameter of 15 mm and length of 110 mm were grown by Czochralski technique and were brought to the indicated sizes by mechanical and chemical handling. A crystallographic direction of a longitudinal axis of the single crystals was <111> and a level of Te-doping was $(2…5)\cdot10^{18}$ cm^{-3}, i.e. $(1…2)\cdot10^{-2}$ atomic %. It allowed within one crystal simultaneously to reveal both types of the impurity inhomogeneities: the striations, and a central impurity core (facet effect). The initial ingots were placed into quartz ampoules with a diameter 30 mm and length 230 mm; the ampoules were pumped out to vacuum not worse than 10^{-4} mm Hg and then were soldered. The methodologies of the single crystalline stocks growing, manufacturing of initial ingots and ampoules, and also treatment of FZM-regimes were explicitly described in [1-3, 7]. In microgravity 2 experiments were carried out. The FZM process began with two-hour holding of the ampoule with a crystal at a given temperature (700–710 °C) on a ring heater that created a melting zone, to reach a steady-state temperature condition of the “Zona-4” furnace. Then the ampoule with crystal moved in relation to the heater on a distance 60 mm with a velocity 5 mm/h. One from experiments was fulfilled under an action on the melt of a longitudinal permanent magnetic field with an induction B = 0.038 T (other conditions were identical). Let's mark that crystals were grown without rotation concerning the heater.

Metodology of study of impuriry inhomogeneities in InSB:Te crystals

Inhomogeneity structure of InSb:Te single crystals was studied by metallography methods along a length of their polishing longitudinal section. The crystals grown in B[$\bar{1}\ \bar{1}\ \bar{1}$] direction were cut along a growth axis at an electrospark (erosive) installation. The section surfaces were grinded using abrasive powders with various sizes of grains down to 5 μm. Then they were polished on cloth using chromium oxide suspension, and were etched in the known modified reagent CP-4 (5 parts of HNO_3, 3 parts of HF, 3 parts of CH_3COOH and 11 parts of H_2O). To develop a thin structure of impurity inhomogeneities the same samples were additionally etched using the special reagent based on potassium permanganate (1 part of HF, 1 part of CH_3COOH and 1 part of aqueous solution

(0.05 M) of $KMnO_4$) during about 3 minutes with a consequent washing in bi-distilled water. Macro- and microstructure of Te-impurity distribution in the specimens was studied using metallographic microscope POLIVAR MET with an attachment of interference contrast according to Nomarski. The specimens were photographed with various enlargements.

To get information on a structure of impurity inhomogeneities, the specimen photos firstly were analyzed visually. The sizes of characteristic details of inhomogeneities were measured; their peculiarities were estimated in space and temporal scales [9]. To obtain reliable quantitative data on periodicity in a structure of the impurity core and striations occurred visually in the sections of the single crystal grown under magnetic field action on the melt, the photos of the polishing sections were numerically coding by computer tools, and a spectral image analysis was carried out [22]. A quantitative analysis of the periodicity revealed in InSb:Te single crystal grown on "Foton-3" by FZM without magnetic field now is under study.

Microgravity environment during Fzm experiments on the "*Fotons*"

Measurements of μg with $f < 0.1$ Hz on "Foton-8" – "Foton-10" using SIY-03 accelerometers showed that these μg continually changed their value and direction; maximum magnitudes were $(7\div15)\times10^{-6}\ g_0$, where $g_0 = 9{,}81\ ms^{-2}$, minimums were $(1\ldots2)\cdot10^{-6}\ g_0$, and during the longest time $\mu g \approx (3\ldots6)\cdot10^{-6}\ g_0$ [14, 15]. Measurements of μg using QSAM and BETA instruments on the "Foton-11" and "Foton-12" [15–17] have confirmed and updated these results.

Based on these data and their mathematical treatment, it is established that the "Foton" type satellites are characteristic with a complicated dynamics concerning the mass center of the spacecraft [15-21]. As a regime of the satellite motion comes nearer to quasi-stationary condition (that usually corresponds to a second half of 14-diurnal flight), the rotation of the "Foton" concerning its mass center becomes more and more similar to Euler regular precession. A simple model to describe it was proposed in [15] for "Foton-11" (Fig. 1).

According to this model, the satellite rotates around X_1-axis directed along a quasi-stationary inertial kinetic momentum with angular velocity $\omega \approx 1$ grad/s (about 1/6 per minute). At the same time X-axis of the satellite moves uniformly around X_1-axis along a cone with a constant opening angle ϑ. Vector $\boldsymbol{\omega}$ moves similarly concerning a XYZ coordinate system. A projection of $\boldsymbol{\omega}$ on X-axis, i.e. an angular velocity of a satellite rotation around its longitudinal axis, is $\omega_1 \approx 0.90$ grad/s; while a projection on YZ-plane, which corresponds to a satellite precession, uniformly rotates around X-axis with a constant angular velocity $\omega_\perp \approx 0{,}17$ grad/s. Approximately the same values were obtained for "*Foton-11*" in [18, 19], and for "Foton-12" in [20, 21].

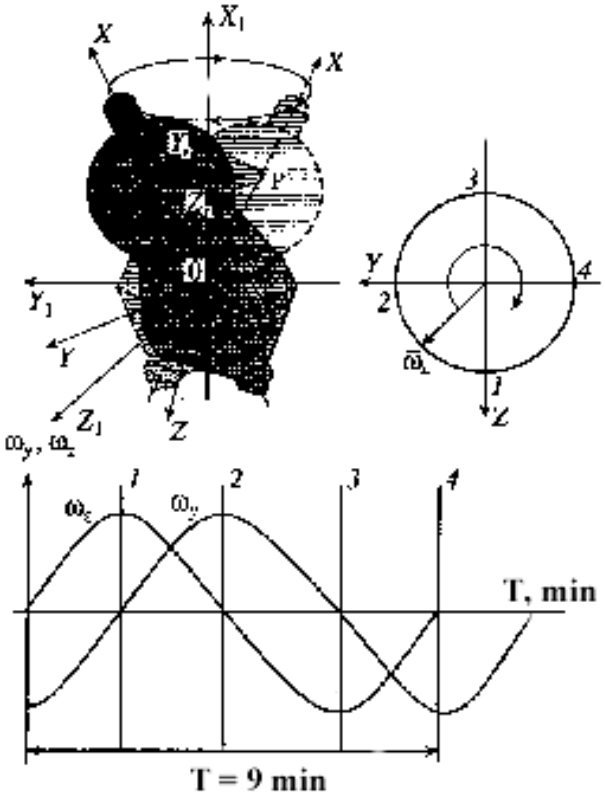

Fig. 1. A model of the "Foton-11" motion about its mass center (a rotation around a longitudinal axis and a precession) [15]. OXYZ is a satellite coordinate system, O is a mass center, P is a place of some instrument location (its mass center). $OX_1Y_1Z_1$ is an orbital coordinate system. ω_i are the angular velocity components in YZ-plane

The regular precession model is available if a satellite is supposed to be an axially symmetric rigid body and if a principal moment of the operating exterior forces is equal to zero. If a satellite is not axially symmetric, the character of a precession will differ from regular a little. In more common case, if a moment of exterior forces is nonzero but small, an inertial kinetic momentum of a satellite can be subjected to displacements, however character of a precession remains close to regular [18-21].

Analysis of microgravity conditions onboard the "Foton-11" and "Foton-12" satellites was carried out using the measured data on μg, on angular velocities of spacecraft, and also on the Earth magnetic field. It was revealed [18, 19] that μg on the spacecraft of a "Foton" series have a number of typing frequencies: f_0 being a frequency of the satellite orbital motion, the frequencies multiple f_0, and others. These frequencies are shown in the left and central columns of Table 1.

As the "Foton" satellites have practically identical design, weight/dimension and starting performances, as well as the similar orbits, their motion in flight appears similar, and so is not surprising, that μg on space vehicle of this type have a similar character. Therefore, we have a sufficient basis to consider μg on the "Foton-3" being of similar performances also.

To analyze experimental results on semiconductor crystal growth from a melt by directional crystallization methods onboard space vehicles, it is necessary

to take into account not only μg, stipulated by satellite dynamics concerning its mass center, but also all other low-frequency (quasi-stationary) actions of small forces on a liquid phase [4–7], i.e. μg of gravity and aerodynamic types. Therefore in [9], using a model shown in Fig. 1 and data on "Zona-4" furnace position onboard "Foton-3", the magnitudes of all μg operating in a mass center of the furnaces were calculated.

Table 1. Frequencies (in 10^{-3} Hz) of harmonic changes of quasi-stationary μg ($f < 10^{-3}$ Hz) on "Foton" type satellites and periodicity in a structure of impurity inhomogeneities of Te distribution revealed in the InSb:Te grown on "Foton-3" by FZM

μg-frequencies in "Foton-11" data measured at the end of flight [18, 19]	μg-frequencies in "Foton-12" data measured at the circuits 16 & 18 [20]	Frequencies in Te-impurity inhomogeneities in InSb:Te crystal [9, 22]
		0.094; 0.122 (≈ $1/2f_0$)
	0.181	0.181 (≈ f_0)
0.197		0.190; 0.197 (≈ f_0)
		0.214; 0.318
	0.331	0.325
0.372		0.366 (≈ $2f_0$)
	0.397	0.397
0.552		0.517; 0.555 (≈ $3f_0$)
0.632		0.665
		0.684; 0.694
	0.761	0.737–0.790
1.012		0.916; 1.020 (≈ $5f_0$)
		1.077–1.313
1.372		1.335–1.413
1.492		1.531
		1.565–1.670
1.862		1.830 (≈ $10f_0$)
		1.938–2.110
	2.167–2.184	2.166
2.229	2.234–2.242	2.212; 2.338
2.509	2.423–2.510	2.380; 2.533
	2.619–2.700	2.756
2.877	2.815–2.872	2.844–2.935
	2.997–3.097	2.970
	3.384–3.753	3.62 (≈ $20f_0$)

Fig. 2 shows dispositions of two "Zona-4" furnaces (No. 1 & 2) on "Foton-3" with the coordinates of the furnace mass centers in $X_CY_CZ_C$ reference frame connected with a satellite mass center (0_C).

Inside each furnace, parallel to its centerline, 3 pairs of ampoules with crystals for experiments were placed symmetrically; the distances between axes of the ampoules within a pair were 260 mm. During FZM process an ampoule moves along positive direction of X_C-axis.

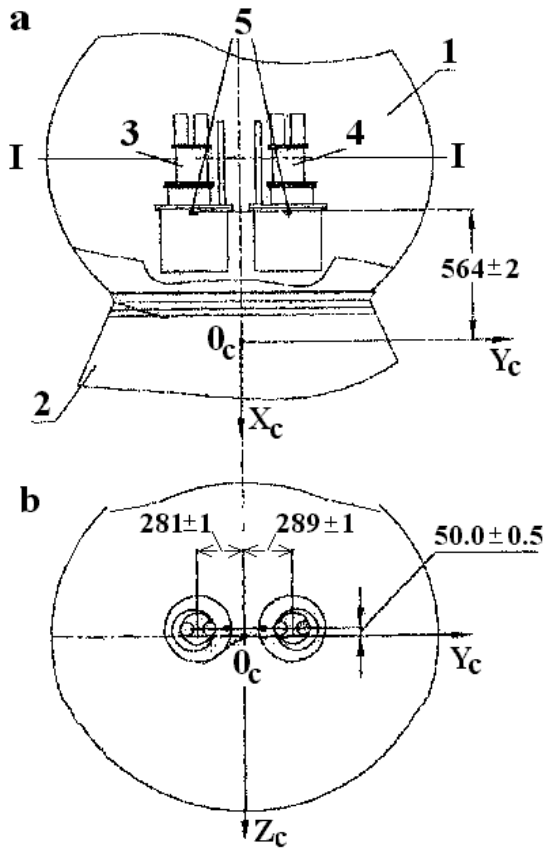

Fig. 2. A scheme of disposition of technological units of "Zona-4" furnaces onboard "Foton-3": a — in X_cY_c-plane (0_c is a satellite mass center); b — in Y_cZ_c-plane along I-I section. 1 is a descent vehicle with scientific payload; 2 is an instrument module; 3 & 4 are "Zona-4" furnaces (No. 1 & 2), 5 are the furnace mass centers (their distances in mm from 0_c are indicated)

Table 2 shows the results of calculations of low-frequency μg, caused as by rotation of the spacecraft around its longitudinal axis and by precession, as by its orbital motion accounting the gravitational and aerodynamic components of μg. The values, depended on satellite dynamics concerning its mass center, do not contradict the results of similar calculations [15] for a location of the QSAM accelerometer on "Foton-11", which were enough well agreed data of low-frequency μg measurements.

Table 2. Micro-accelerations at the mass center of "Zona-4" furnace onboard "Foton-3" satellites (calculations)

Causes of mg	Constant components		Amplitudes of harmonic components	
	Transversal	Longitudinal	Transversal	Transversal
Rotation around a satellite mass center	$10^{-6}g_0$	$\approx\geq 8\cdot10^{-6}g_0$	$3\cdot10^{-6}g_0$	$10^{-6}g_0$; $2\cdot10^{-7}g_0$
Gravitational	–	–	$2\cdot10^{-7}g_0$	$3\ 10^{-8}g_0$
Aerodynamic	–	–	In perigee $2{,}4\cdot10^{-7}g_0$; In apogee $6{,}4\cdot10^{-9}g_0$	In perigee $1{,}4\cdot10^{-6}g_0$; In apogee $3{,}6\cdot10^{-8}g_0$

Results and discussion

As it is known (see, for example, [11, 23]), one of the main characteristics of FZM process in microgravity should be development in a melt of Marangoni convection (thermal- and/or solutal-capillary), which prevails above possible flows driven by buoyancy. When convection is non-stationary an origin of striations is expected.

The photos of structure of the polishing longitudinal sections of the InSb:Te single crystals, grown by FZM in flight of the "Foton-3" satellite, are given in Fig. 3 [1–7].

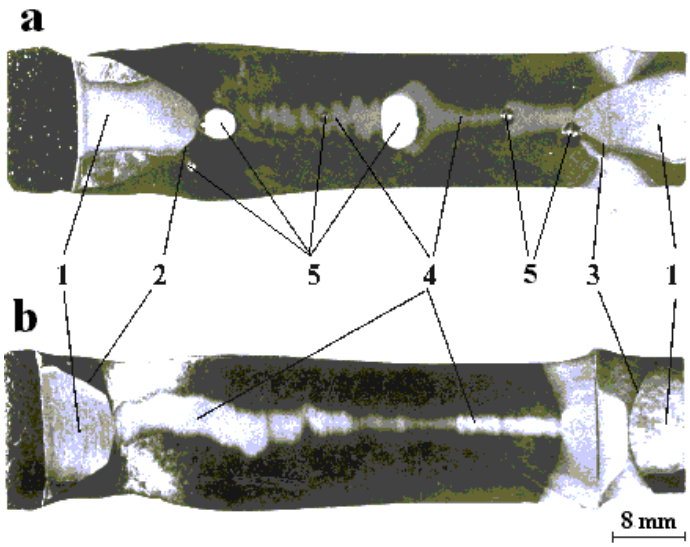

Fig. 3. A structure of the polishing longitudinal sections of InSb:Te single crystals grown by FZM on "Foton-3": a — under the action of magnetic field with induction B = 0.038 T; b — without magnetic field. 1 is an impurity core (the facet effect) in the initial single crystalline InSb:Te ingots; 2 & 3 are the melt boundaries in the initial ingots at the beginning (2) and at the end (3) of FZM; 4 is the impurity core within the single crystal parts re-crystallized during a flight; 5 are gas pores

This Figure first of all takes our attention to unusual character of behavior of the impurity core (the facet effect) in both crystals: change of its size and positions about a longitudinal axis of crystal (the lighter areas correspond to the greater concentration of tellurium). A similar structure of the impurity core was not observed in InSb:Te crystals growing on the Earth by Czochralski technique.

The specific interest calls the single crystal grown under an action of magnetic field: in this crystal the behavior of the impurity core have an explicitly expressed quasi-periodic character (see Fig. 3a).

This crystal has given a possibility to study two aspects of impurity inhomogeneity: the facet effect and striations, which formed simultaneously, independently from each other and under different laws. Besides, the gas pores are also detected; they centered, in basic, near a longitudinal axis of the crystal.

Apparently, the magnetic field, despite of a rather small, could in a defined degree stabilize and order the convective flows in a melt that promoted keeping of bubbles hampering their departure from a melt.

The visual analysis of Fig. 3a has shown that a period of the impurity core changing is close to $T_0/3$, where $T_0 \approx 90$ minutes is an orbital cycle time of the "Foton" spacecraft (an orbital frequency $f_0 \approx 1{,}85 \cdot 10^{-4}$ Hz). Really, the velocity of the capsule with crystal motion (which is approximately appropriate to growth rate) was equal 5 mm/h or 0.08(3) mm per minute, and the distance between maximums of the impurity core displacement concerning the crystal longitudinal axis is about 2.2 mm on the average. It signifies that the time it takes for increasing of the crystal length of 2.2 mm, and consequently, an average period of the impurity core oscillations are equal 26.4 minutes (the corresponding frequency $6{,}3 \cdot 10^{-4}$ Hz that is approximately 3,4 times more than f_0) [9].

It was shown in [4–7] that the most probable reason of considered anomaly origin is the action on a melt of quasi-stationary residual μg having the component which is orthogonal to crystallization direction and changing its magnitude and direction. In the same papers the physical model was offered, according to which these μg, i.e. the small forces of gravity and inertial nature, break a symmetry of fields of convective flow, temperature and concentration in the melt. It results in displacement of a crystallization boundary isotherm concerning a longitudinal axis of the melting zone, and because of it to a corresponding displacement of the facet effect in a growing crystal. Numerical simulation (within the simplified 2D-model [5]) had shown that the isotherms in a melt displaced sideways along an operating constant acceleration, transversal to crystallization direction, even if it was small (from 10^{-4} to $10^{-8} g_0$).

Fig. 4 demonstrates a part of the longitudinal section of the crystal shown at Fig. 3a with a large magnification, in which both the impurity core, and striations are well visible.

For the first time it was observed that striations grouped into the "packages" containing tens stratums, with a package width close to ~1 mm; the space periodicity of package sequences corresponded to those periodic changes of the impurity core position (i.e. approximately 2…2,5 mm). It signifies that the packages of striations also alternated with a time interval close to $T_0/3$ [8, 9]. It allows to conclude that the formation of striation packages, as well as anomalous behavior of the facet effect, is connected with the changes of intensity and direction of convective flow in the melt under an action of quasi-stationary μg varying their magnitude and direction. The convective flows cause the concentration and temperature inhomogeneities both in volume of the melt, and in a boundary layer near to crystallization front that generates macro- and micro-inhomogeneity of impurity distribution in the growing crystal [12]).

Inside the packages it is possible to distinguish more small-sized subgroups of striation, approximately 5-6 in each package with a subgroup width about 0.2 ~ mm. The space periodicity of alternation of subgroup sequences "lighter + darker" is about 0.4 mm. It gives an evaluation of temporal periodicity of subgroup alternation as approximately 4.8 minutes that is close to a half-period of the "Foton" rotation concerning its mass center which is equal about 9 minutes. The resolution of a photo shown at Fig. 4 does not allow making such calculations

sufficiently confidently basing at the visual analysis. However digitization of brightness of an image at Fig. 4 by the computer tools and the consequent spectral analysis [22] have allowed to select a lot of frequencies in Te-distribution as in the impurity core as in striations. It turned out that these frequencies practically coincided with the frequencies of μg measured onboard the "Foton" type satellites (see a right column in a Table 1).

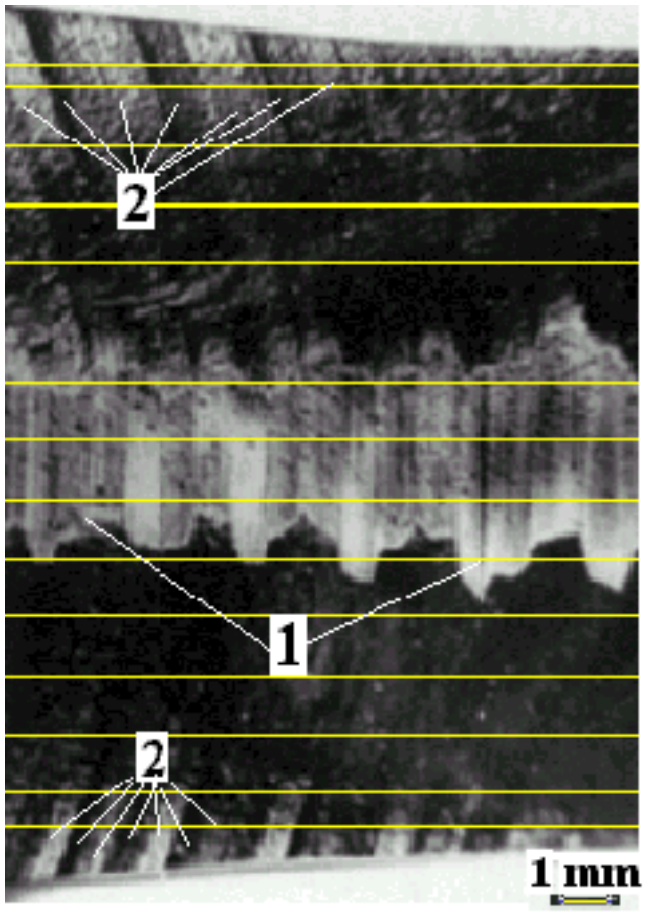

Fig. 4. An enlarged fragment of microstructure of the longitudinal section of the InSb:Te single crystal, shown on a Fig. 3a. 1 is the impurity core, 2 are the striations with a complicated structure: they are grouping into "packages", inside which the subgroups are distinctive also. Horizontal directs are the lines, along which a numeric encoding of an image was made

In Fig. 5 a part of the same longitudinal section of crystal is shown with further more magnification. Noticeably that within a scale segment of 50 μm in length approximately 4–6 striations are occurred; it corresponds to a distance between them from 12.5 to 8 μm. The estimations of a time period (T_{fl}) and a frequency (ν_{fl}) of the alternation at Fig. 5 give $T_{fl} \approx 9\ldots6$ s, $f_{fl} \approx 0.11\ldots0.16$ Hz [9], and a frequency revealed by spectral analysis is 0.13 Hz [22]. According to existed representation [23] these magnitudes correspond to a period and a frequency of temperature fluctuations of Marangoni convective flow in a melt, which is responsible for a thin structure of striations in the growing crystal.

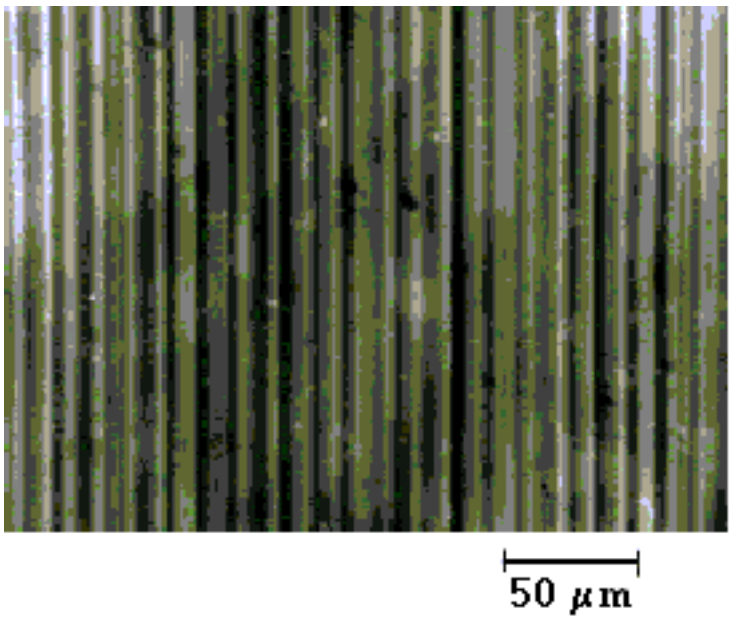

Fig. 5. An enlarged fragment of microstructure of the longitudinal section of the InSb:Te single crystal, shown at Fig. 3a. Thin stratified structure of the impurity striations is revealed

The variety of the frequencies of μg onboard the "Foton" type satellites and the frequencies detected in distribution of impurity in the grown InSb:Te single crystal, apparently, is explained to that the μg spectrum contains not only the frequencies caused by orbital motion of a spacecraft, its rotation around an axis of a principal moment of inertia and precession, but also the multiple frequencies, as well as the frequencies of summarized coherent and/or non-coherent harmonic oscillations. Besides, the μg spectrum can include the quasi-periodic oscillations also having a line spectrum of frequencies.

Physically it is quite explained that, under an action of periodic changes of direction of a low-frequency μg vector, the smooth changes happen in the fields of concentration and/or temperature in the melt, and these inhomogeneities are recorded spiral-like by the growing crystal. The magnitudes of these μg generally exceed 10^{-7} g_0; therefore in all experiments on semiconductor single crystal growth by directional crystallization methods, which carried out on space vehicles, until now it was not possible to obtain the perfect uniform crystals. In [12] it was shown that, when a ratio of length to diameter of the melt area is about 4 (it is characteristic for a main part of crystal growth experiments in microgravity), such values of μg provide for intensity of convective flows in the melt corresponding to Rayleigh numbers $Ra > 0.01$. Such flows lead to an origin of inhomogeneities in the fields of concentration and/or temperature as in the melt volume as near crystallization front. It results in segregation and inhomogeneities of the component distribution in the growing crystal.

Microgravity environment onboard the "Foton" type satellites, being complicated on frequencies and amplitudes of μg, has resulted in a complicated picture of impurity inhomogeneities in the grown InSb:Te crystal. The adequate mathematical model, which is capable to describe action of all frequency bands of

μg on the melt, now does not exist. To create such model, it is necessary to realize some specially prepared experiments in inspected μg-conditions on space vehicle, and also to fulfil numerical simulations of heat/mass transfer in a melt in a statement of problems adequate to actual processes and technological conditions of crystal growth.

Conclusion

In the InSb:Te single crystals grown by FZM on the "Foton-3" satellite the periodic changes in distribution Te-inhomogeneities as impurity core (facet effect) and striations were detected. This periodicity is a consequence of action on the melt of variable on magnitude and direction low-frequency microaccelerations.

The results of measurements and calculations of quasi-stationary (with frequencies $f < 5 \cdot 10^{-3}$ Hz) micro-accelerations, caused by a complicated flight dynamics of the "Foton" type satellites, are systematized and analyzed. Micro-accelerations practically exceed values of $\mu g \sim 10^{-7} g_0$. Such forces are sufficient for origin of inhomogeneities in the fields of convective flow, temperature and concentration in the melt, and, accordingly, for segregation and inhomogeneity of impurity distribution in the crystals, growing by directional crystallization of melts.

The periodicity in a character of distribution of doping impurity as striations, and also in behavior of impurity core, which were revealed in the InSb:Te single crystals grown on the "Foton-3", practically coincide with the frequencies of quasi-stationary micro-accelerations, characteristic for the "Foton" type satellites. It proves that the reason of origin of indicated periodicity really are the variable on magnitude and direction residual micro-accelerations onboard the satellite, defining the fields of flow, temperature and concentration in the melt. It confirms physical representations about influence of small forces of a gravity and inertial nature on the processes of segregation during directional crystallization of melts.

3.2.2. DEVELOPING OF NEW METHOD OF CRYSTAL GROWTH IN MICROGRAVITY

A new method of crystal growing in space (contactless directional crystallization-CDC) is proposed and substantiated. The method represents a combination of advantageous features of the Bridgman method and the floating zone technique. The basic idea consists in obtaining the melt configuration that does not contact the latteral walls of a cylindrical ampoule and has a free surface pinned to the edges of end plates. The shape and stability of an isothermical capillary liquid with the configuration outlined above have been analyzed for cases of zero-gravity, an axial gravity and a lateral gravity. It has been shown, that the region of stable configurations depends essentially on melt wetting angles with the cylindrical walls and with the end plates. Wetting angles of liquid Ge and GaSb of different materials were measured and found ones, suitable for realization CDC. It was performed design of ampoule for growth of GaSb in space by CDC method.

Description of the method

Contact of a melt with the lateral ampoule walls has detrimental effects on the structure of growing crystals, because they produce undesirable stresses. A new

idea on crystal growing in space consists in an optimal combination of elements of the Bridgman method and the floating zone method of crystal growth [1]. On the one hand, it is necessary to retain an ampoule to prevent melt spilling. On the other hand, it is desirable to have a free surface that does not contact the cylindrical walls. Thus, the goal is to obtain the melt configuration that represents a "liquid bridge" inside an ampoule with a free surface pinned to the edges of end plates (Fig. 1).

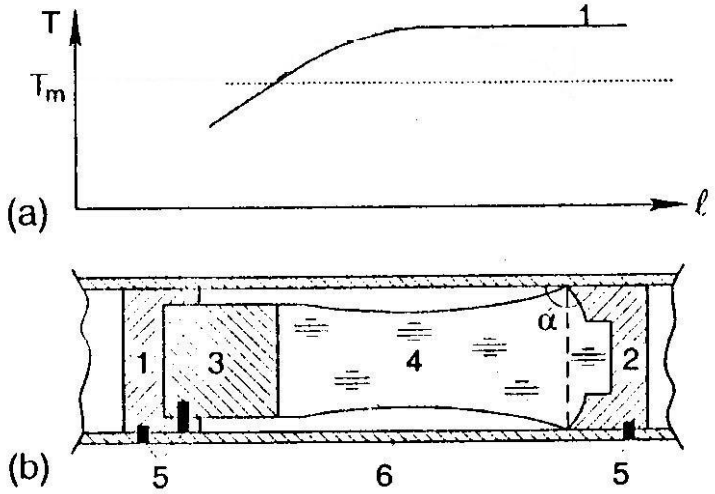

Fig 1. Scheme of a growth experiment. (a) Temperature distribution along the ampoule (T_m = melting temperature). (b) Diagram of the cartridge: (1) seed support; (2) support wetted by the melt: (3) seed; (4) initial melt configuration; (5) pins for support and seed; (6) container

Such a configuration is always unstable for a cylindrical container with uniform value of the wetting angle. It may be stable only if the cylindrical walls are unwetted, and both ends of an ampoule are wetted [2, 3]. Because of this, it is suggested to make one end of the ampoule from a material that is well wetted by the melt (e.g., quartz is wetted by germanium). The other end of the melt zone is in contact with a single crystal seed plate. There is a complete wetting here since melt always wets the same solid material.

Shape and stability of liquid bridge between wetting ends of a cylindrical ampoule

Stability conditions. Among the problems that are to be solved first for devising this method, one must consider the shape and stability of the free surface. First, it is necessary to provide the liquid bridge stability just after melting, i.e. for the total length in liquid form. The stability criterion for the system under consideration reduces to the following [2, 3]:

a) the bridge must be stable under perturbations that preserve the liquid volume and retain the contact lines pinned to the edges of end plates;

b) the dihedral angles Ψ_1 and Ψ_2 (Fig. 2) formed by the melt along the edges, must satisfy the conditions:

$$\alpha_1<\Psi_1<\alpha-\pi/2, \quad (1)$$

$$\alpha_2<\Psi_2<\alpha-\pi/2. \quad (2)$$

Here, α, α_1 and α_2 are the *wetting* angles of a melt at the contact with *smooth* solid surfaces of the lateral wall, upper and lower ends, respectively.

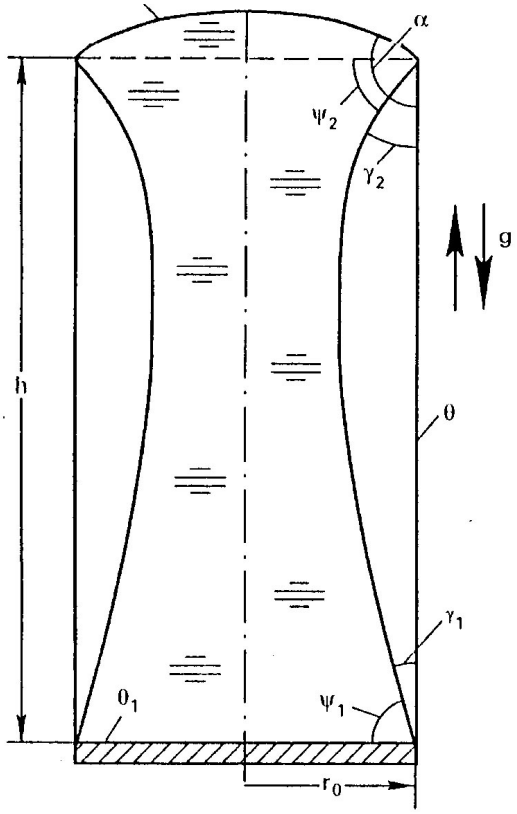

Fig. 2. Sketch of an axisymmetric liquid zone inside a cylindrical ampoule with wetting ends

The inequalities (1) and (2) provide the stability conditions with respect to perturbations that displace the contact lines from the edges. When these inequalities are fulfilled, the most dangerous perturbations are restricted to those described in the item a).

Below we analyze these stability conditions for zero-gravity, for an axial steady gravity and for a lateral steady gravity (Fig. 3). Apart from the wetting angles α, α_1 and α_2, the stability of the melting zone is described by the slenderness (aspect ratio), Λ, the relative volume, V, and by the Bond number, B. They are defined as

$$\Lambda = h/(2r_0),\ V = \nu/(\pi r_0^2 h),\ B = \rho g r_0^2/\sigma \quad (3)$$

Here, r_0 and h are the cylinder radius and height, and ν, ρ and σ are the liquid volume, density and surface tension, respectively. Except for the case $g = 0$, we consider the most dangerous (for the space conditions) level of axial ($g = g_a$) and lateral ($g = g_l$) gravities that is estimated as $g = 0.01 g_0$ ($g_0 = 9.81$ m/s^2). Assuming that $r_0 = 0.75$ cm and using the physical properties of Ge and GaSb at their melting points, we estimate the axial (B_a) and lateral (B_l) Bond numbers as those equal to 0.05.

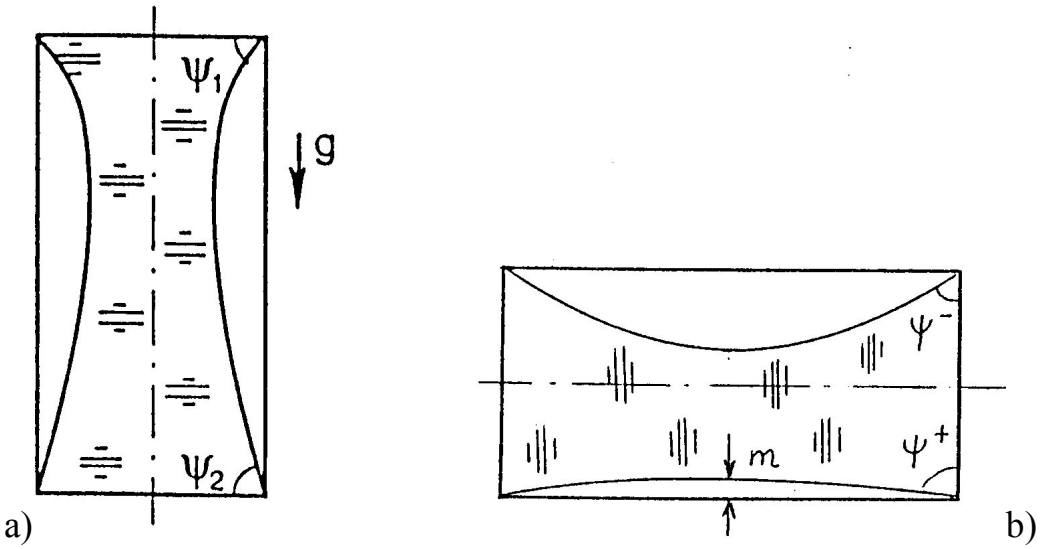

Fig. 3. Sketch of a liquid zone inside a cylindrical ampoule with wetting ends: (a) axial gravity; (b) lateral gravity

A conclusion about the stability of such a bridge under perturbations described above in item a) can be drawn using results published in [3–4]. The related stability regions for $B = 0$, $B_a = 0.05$ and $B_1 = 0.05$ are shown in Fig. 4. They are presented in the (Λ, V)-plane. Each region is bounded from below by the corresponding solid line. These lines merge at small values of Λ. We consider only part $V < 1$ of the stability region corresponding to bridges inside the cylinder.

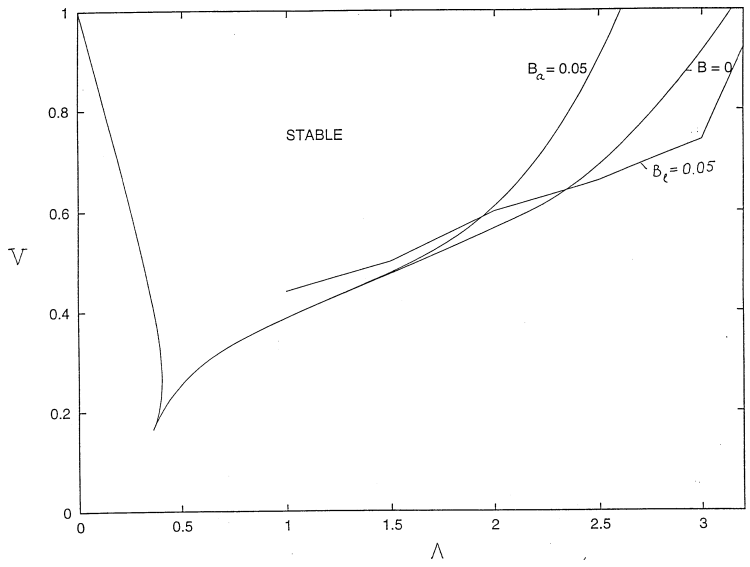

Fig. 4. Boundaries of the stability region under perturbation remaining the contact lines on the edges of end plates for $B = 0$ (after [3, 4]), $B_a = 0.05$ (after [5]) and for $B_1 = 0.05$(after [6])

Liquid bridges that belong to the constructed regions are stable only under perturbations remaining the contact lines on the edges. To be stable to arbitrary perturbations, bridges must satisfy additionally the inequalities (1) and (2). Below we present numerical data that allow an separating the states that are stable to

arbitrary perturbations. We will call the related region of the *(*Λ, *V*)-plane as a general stability region.

For zero-gravity conditions, $\psi_1 = \psi_2 = \psi$. The dashed lines in Fig. 5 represent the level lines $\psi = const$ inside the stability region for $B = 0$. Points of each dashed line correspond to bridges with one and the same value of ψ. The line $\psi = 0$ coincides with the left-hand segment of the stability boundary for perturbations remaining the contact lines on the edges. Each line $\psi = const$ touches the right-hand segment of the stability boundary. The level lines $\psi = const$ allow one to construct the general stability region. Let, for example, $\alpha_1 = 30°$, $\alpha_2 = 0$ and $\alpha = 150°$. Then, according to (1) and (2), the bridge is stable if and only if its parameters Λ and *V* belong the general stability region bounded by the lines $\psi = 30°$ and $\psi = 60°$.

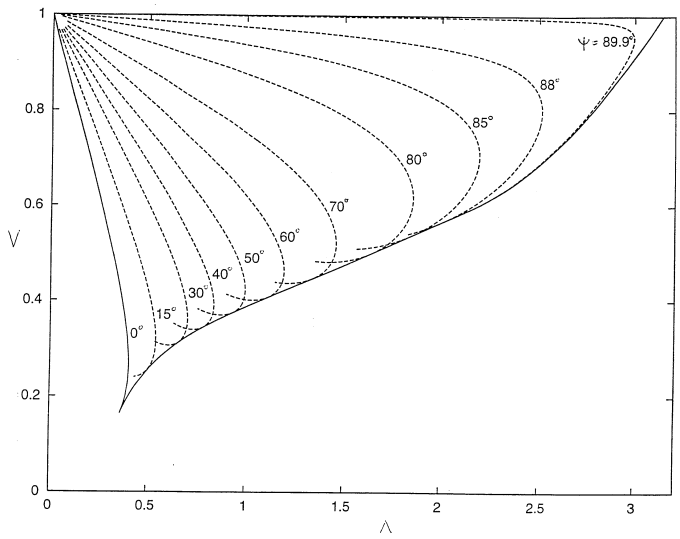

Fig. 5. Stability boundary (solid line) for a weightless liquid bridge pinned to the edges and the level lines$\psi = const$ (dashed lines)

For an axial gravity, the ψ_1 and ψ_1 values for a fridge are related by the equation [5] $\sin\psi_1 = \sin\psi_2 - \Lambda B(1 - V)$, so that $\psi_1 < \psi_2$. The level lines $\psi_1 = const$ and $\psi_2 = const$ inside the stability region for $B_a = 0.05$ are shown in Fig. 6. The lines $\psi_1 = a$ and $\psi_2 = a$ with a small *a* practically coincide with the line $\psi = a$ for the case of $B = 0$. This is why the lines $\psi_1 = 15°$ and$\psi_2 = 15°$ are replaced in Fig. 4 by the line $\psi = 15°$. All the lines $\psi_2 = a$ $(0 < a < 90°)$ touch the right-hand segment of the solid stability boundary. However, for the lines$\psi_1 = a,$ this is true only at the *a* values up to 73.5°. The value 73.5° is the maximum value that the angle ψ_1 reaches along the stability boundary for perturbations remaining the contact lines on the edges. For the corresponding state, $\psi_1 = 73.5°$ and $\psi_2 = 90°$. If $73.5° < a < 90°$, the level line $\psi_1 = a$ ends at the point of intersection with the line $\psi_2 = 90°$. The points that lie beyond the line $\psi_2 = 90°$, i.e. in the region bounded by the lines $\psi_2 = 90°$, $V = 1$ and the stability boundary for $B_a = 0.05$, correspond to states with $\psi_2 > 90°$. These states can not exist inside a cylinder.

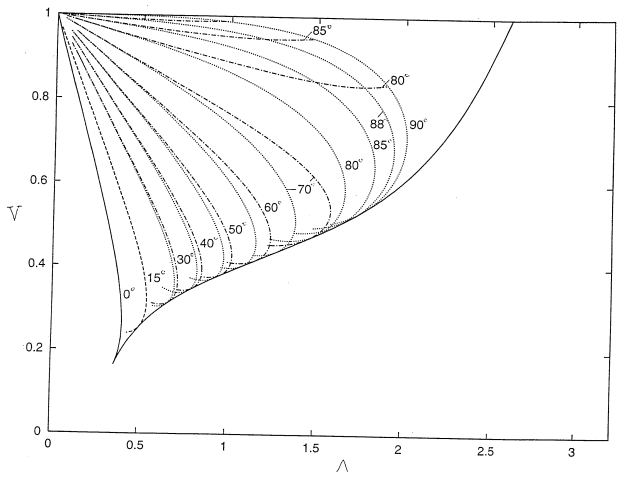

Fig. 6. Stability boundary (solid line) for a liquid bridge pinned to the edges and the level lines $\psi_1 = const$ (dot-dash lines) and $\psi_2 = const$ (dotted lines) in the case of the axial Bond number $B\% = 0.05$

Let α^+ be a larger of the values α_1 and α_2, and α — be a smaller one. Since $\psi_1 < \psi_2$ and a gravity may by directed either to the plate end with the wetting angle α_1 or, alternatively, to the end with the wetting angle α_2, the inequalities (1) and (2) reduce to the following:

$$\alpha^+ < \psi_1 \text{ and } \psi_2 < \alpha - \pi/2. \tag{4}$$

Let us consider, as an example, the previous values $\alpha_1 = 30°$, $\alpha_2 = 0$ and $\alpha = 150°$. Then, according to (4), the general stability region in the (Λ, V)-plane is bounded by the stability boundary and by the level lines $\psi_1 = 30°$ and $\psi_2 = 60°$. For the example under consideration, the general stability regions for the cases $B = 0$ and $B_a = 0{,}05$ are shown in Fig. 7. We see that the general stability region under an axial gravity lies inside the region for zero-gravity, as expected.

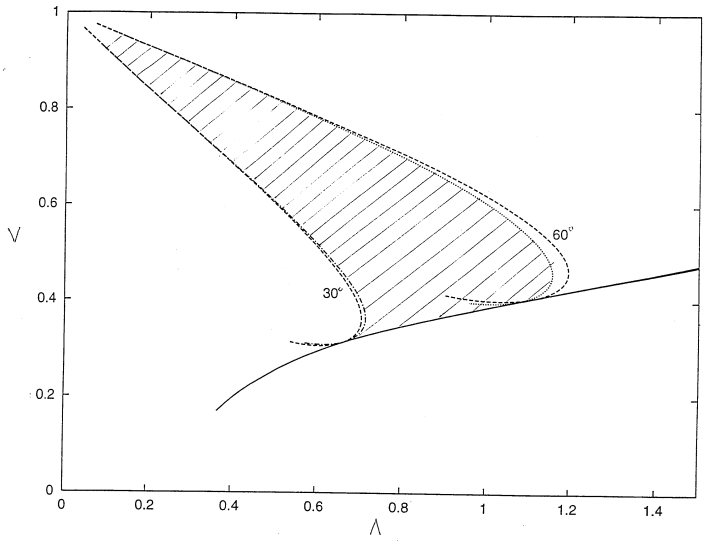

Fig. 7. General stability region for $\alpha_1 = 30°$, $\alpha_2 = 0$ and $\alpha = 150°$ in the cases $B_a = 0.05$ (shaded region) and $B = 0$. The line styles are the same as in Figs. 5 and 6

For the case of a lateral gravity, the liquid bridge shape and stability problem becomes much more difficult owing to nonaxisymmetry of the shape. The solution procedure for the problem and examples of critical shapes and stability boundaries under perturbations satisfying the conditions a) are presented in [6, 7]. In this case, $\psi_1 = \psi_2 = \psi$ but the angle ψ is no longer constant along the contact lines. A maximum value, $\psi = \psi^+$, and a minimum value, $\psi = \psi^-$ are reached at the bottom and the top points of the contact line, respectively. The inequalities (1) and (2) assume the form

$$\alpha^+ < \psi^- \text{ and } \psi^+ < \alpha - \pi/2. \quad (5)$$

In addition, it is necessary to analyze the shape of a stable bridge to provide the conditions under which a molten zone does not contact a middle part of lateral walls, i.e., a distance *m* is non-zero (see Fig. 3b).

Measuring of wetting angles of liquid GaSB and Ge of solid GaAs and Si accordingly

Thus we have some abstract mathematical simulation of stability conditions for large bulk of melt, suspended in weightlessness without contact with container walls. For realization of this process in space it is necessary to find materials with suitable values of wetting angles by molten zone end face and container.

There is no problem to find materials that are not wetted by liquid Ge and GaSb (wetting angle value more, than 130 degr.). It may be silica (after special treatment), graphite and so on.

Evaluation literature data on the wetting angles of semiconductor melts to various substances revealed, that it is very difficult to find materials with wetting angles < 70 degr.

We decided to use for this purpose (as end plate or face) similar semiconductors (for example: Si for Ge and GaAs for GaSb), which have significant higher melting temperature, and don't change electrophysical properties of Ge or GaSb, because Si in Ge and As in GaSb are the electrically neutral (inactive) impurities.

We measured wetting angles solid Si by liquid Ge and solid GaAs by liquid GaSb [8]. For this purpose, we depose Ge or GaSb on the horizontal plate wafers of Si or GaAs, melt Ge or GaSb and investigate the picture of the melts.

We obtained the following values for: solid Si by liquid Ge (T = 950–980 °C) –32°(vacuum ~ $l0^{-4}$Hg), and –31° (Ar, lat); for solid GaAs by liquid GaSb (T = 720–780 °C) –34°(vacuum ~ $l0^{-4}$Hg).

In these cases, it is possible to use these materials (GaAs and Si)as end plate or fase. The measure of distribution of Si or As along grown crystal Ge or GaSb give additional information about heat-masstransfer in melt Ge or GaSb in space conditions.

After these mathematical simulation and experimental investigation it is clear, how to realize concrete process of CDC of Ge and GaSb in space and it was possible to begin the real Ground Testing of CDC Method.

On-ground treatment of CDC method for GaSb

We designed the construction of ampoule (Fig. 8) [9, 10]. We use special graphite compressed spring. The peculiarity of this construction is the limitation of moving GaAs — plate aside GaSb — melt with the help of special restrictor.

Such ampoule didn't destroy after vibration and stock testing (Their value were the same for launch and land spacecraft.)

We prepare samples for experiments on the "Polyzon" growth furnace on the board of automatical station "Foton".

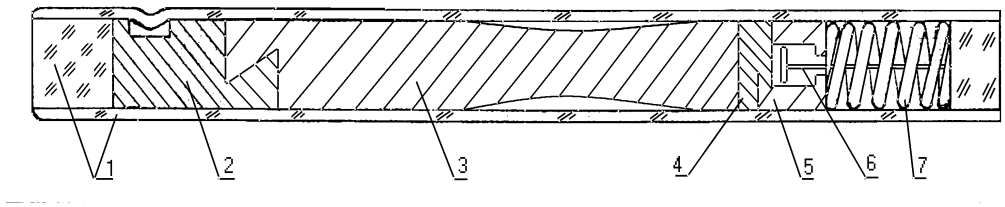

Fig. 8. Scheme of cartridge for real experiment in space: 1 — silica plugs and container; 2 — graphite seed part of GaSb support; 3 — initial GaSb ingot; 4 — GaAs end plate; 5 — graphite GaAs support; 6 — restrictor; 7 — graphite compressed spring

Conclusion

The new method of a directed crystallization in space has been suggested. The investigation of the equilibrium shape and stability problems for an isothermical capillary liquid with a free surface pinned to the end edges has been performed for the cases of zero-gravity, an axial gravity and a lateral gravity. It has been shown that the region of stable configurations depends essentially on the melt wetting angles with the cylindrical walls and with the end plates. The results of the investigation justify the reality of the method employment. The recommendations on the length of melting zone and the volume of a solid sample that have to be melted have been obtained. We found material for end plate, suitable for realization CDC GaSb in space. It was designed ampoule and performed on ground treatment of this experiment.

3.2.3. EFFECTS OF MELT STRUCTURAL SELF-ORGANIZATION WITHIN THE TRANSIENT LAYER DURING CRYSTAL GROWTH IN MICROGRAVITY

A brief review is given of the results obtained in 2003–2005 by IChPM and IPPE during their joint study and modeling of Ge:Ga, Ge:Sb, GaSb:Te, InP:S single crystal growth from stoichiometric and non-stoichiometric melts on board the *Photon* satellite series. The use of microgravity is shown to be justified and holding promise for research into the structural self-organization processes (cluster forming) taking place within the transient layer of the melt during the solidification. This is the first time that a mathematical model of convective heat and mass transfer taking into account the double-phase character of matter in the boundary layers near the interface has been created and used as an independent tool for the study of such processes. Prospects are discussed for this new area of the space material science.

Introduction

The IChPM research strategy consists in the purposeful use of microgravity as a specific physical environment to solve fundamental problems related to study and mathematical simulation of the processes taking place during semiconductor and multicomponent intermetallic compound crystallization from a liquid phase. Zero-gravity is an ideal unperturbed environment for study of fundamental phase transition mechanisms under conditions where the uncontrolled influence of any external forces upon the crystallization system is extremely low.

The number of on-board technological experiments has decreased sharply in recent years due to the sinking of the *Mir* space station (2001), the failed *Photon-M1* launch (2002) and the *Columbia Space Shuttle* accident (2003). In this context the IChPM turned to ground-based development, perfecting and refining of technological processes planned for the *ISS* and *Photon-M2* missions and to analysis of the previous on-board semiconductor single crystal growth experiments data.

In 2003–2005 the financial support for this study was obtained from the Russian Foundation for Basic Research (RFBR) Grant #03-02-16282 "*The effects of structural ordering in melts within the interface area at the doped semiconductors single crystal growth in microgravity*" and the EC-ESA NMP-CT-2004-500635 contract in the framework of "*Intermetallic Materials Processing in Relation to Earth and Space Solidification* (*IMPRESS*)" Integrated Project of Europe's FP6 program [1].

The experimental results accumulated over many years led us to conclude that in the on-board crystal growth one needs to take into consideration the phase and structural state of the transient *delta*-layer in order to be able to account for doping anomalies and specific intrinsic defects in space-grown crystals. Among other things we came to the conclusion that we should describe the structure of the boundary *delta*-layer in terms of clusters.

The research on material structural transformations during phase transitions at temperatures near the melting temperature range is essential to the understanding of fundamental processes and mechanisms of crystallization. Actually, in a modern material science there are not any fundamental problems in either elucidating the structure and properties of single crystals being obtained or describing and modeling hydrodynamics and heat/mass transfer in the bulk of a melt during the crystallization process. The state of matter in the narrow boundary region at the interface and the heat/mass transfer processes in the precrystallization layer appear to be the only unsolved problem left. The difficulty of investigating this problem is aggravated by the fact that during "terrestrial" crystal growth processes the transient region has very small dimensions (tens/hundreds of micrometers) and the side facing a melt is destroyed permanently by natural and/or artificially created convective flows. Since the melt structuring phenomena in the transient layer are extremely susceptible to exposure to any energy, like thermal, mechanical (mixing, vibration), electromagnetic, gravity forces etc., the ideal environment where they manifest themselves and can be studied is the state of microgravity realized aboard an orbital vehicle.

Results and discussion

The unique hydrodynamic and thermal conditions characterized by extremely weak convective mixing of the melt are formed under the influence of residual gravitational field which is reduced 10^6 times at an altitude of 300–400 km in a near-earth orbit. During zero-gravity crystallization processes the thickness of the near-interface transition layer in the melt reaches 3–6 mm [2, 3]. The formation of ordered groups of atoms responsible for short-range ordering in the melt changes the structure-dependent properties of this extensive precrystallization region (viscosity, density, thermal conductivity, hydrodynamic resistance etc.) as well as the local coefficients for dopant distribution at the interface. The fundamental structuring phenomena determine to a large extent the character of heat and mass transfer in the interface region and have a very strong effect upon the crystallization mechanism as a whole, because the thermogravitational convection is extremely small whereas the size of the phase inhomogeneity region is significant. This in its turn accounts for dopant distribution anomalies and anomalies of electrophysical properties experimentally detectable in the semiconductor solid phase as well as for specific intrinsic structural defects in multicomponent compound crystals being grown.

As the part of preparatory stage of work the analysis was performed of the effect of gravitational modes of "Mir" station's orbital flight upon semiconductor crystallization processes with Ge float zone melting used as an example [4]. It was demonstrated experimentally that the non-stationary thermogravitational convection in the melt will only become negligible when the microgravity level is $4 \cdot 10^{-6}$ of its on-the-ground value (g_0) or less. Which is why we were focusing on the comprehensive study of the single crystals obtained during the seven "Foton" unmanned explorer missions under extremely low level of residual microgravity of about $3 \cdot 10^{-6} g_0$.

Experimental and theoretical study was made of structural ordering processes (cluster forming) within the melt transient region near the growing crystal interface. The subject of the study was the processes of crystallization and doping of elementary semiconductors (with Ge:Ga, Ge:Sb used as examples) as well as binary semiconductors of the A_3B_5 group (we used GaSb:Te, InP:S as examples) from the liquid phase (melt) under extremely low microgravity. Single crystals of these materials (see examples in Figure 1) were grown by float zone melting and traveling heater methods with the use made of the orbital growth equipment "Zona-4" developed by Design Bureau of General Machninebuilding (DBGM or KBOM). Complex characterization of the semiconductor crystals was carried out using *state of the art* analytical techniques. A concept was used where crystals being grown were looked upon as a sort of "photographic pictures" of the transient interfacial layer state. Particular attention was given to study of regions adjacent to the initial crystallization front (seeding front). Data of single crystal impurity, electrophysical and structural inhomogeneity analyses were used as independent benchmark results to verify numerical model calculations. It was shown that the fundamental effects of melt structure ordering in space are most conspicuous in the pre-crystallization region at temperatures near the melting

point, where the intensity of convective mixing, smoothing the layer adjacent to the crystallization front and destroying cluster formations is close to zero [5].

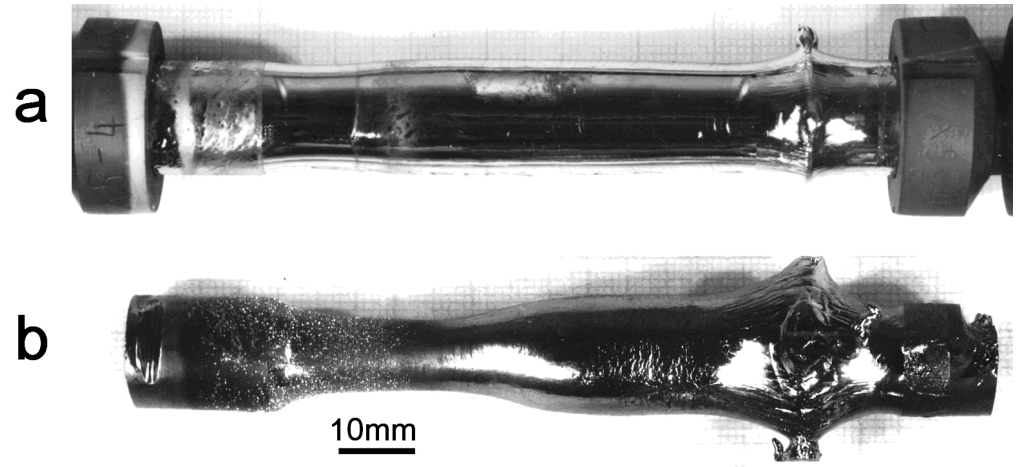

Fig. 1. Samples of single crystals grown by Float Zone Melting method onboard *Photon* satellites: a — Ge:Ga; b — GaSb:Te. Courtesy: GIREDMET (V.V. Rakov)

The calculational powers of the SSC RF Institute for Physics and Power Engineering (IPPE) computer stations were used for numerical studies and simulations. A number of significant new results were obtained. A new version of mathematical model for convective heat and mass transfer including hydrodynamics equations and equations for impurity transfer and convection flows in the transient region was specially developed for the first time to be used as the independent tool for study of structural self-organization processes (clustering) in boundary layers [6]. The model design is distinguished by its novel approach to conjugated hydrodynamic and crystallization processes description. It allows the description of the melt crystallization process with due consideration of the moving interface, convective heat/mass transfer and impurity segregation. This is the first time such a model has taken into account the structural pre-crystallization state of the boundary layer at the interface. For the first time the transient region is described as a double-phase medium containing apart from the melt volumetric cluster formations impeding the flow [7].

In the study of "orbital" Ge:Ga, GaSb:Te and GaSb:In single crystals the value of *alpha*, the "clustering constant", was estimated in stoichiometric doped melts of Ge and GaSb. *Alpha* is included in the mathematical model we developed as a key parameter and implicitly characterizes the shape and average size of the solid phase clusters formed in the transient layer at the crystallization front. Physically *alpha* depends on the "surface/volume" ratio of the germs of the solid phase offering resistance to the laminar melt flow washing the crystallization front. It is shown that for Ge and GaSb this parameter "*alpha*" is conservative enough and as a first approximation it does not depend on the dopant type been ranging from $6.2 \cdot 10^{17}$ to $7.0 \cdot 10^{17}$. For a numerical estimate we were the first to use the effect of concentration stratification of the melt caused by a stationary residual gravitation vector as a test physical process [8]. The cluster forming process near

the crystallization front is shown to be actively proceed in the area bounded by isotherms $]T_{melting};T_{melting}+10K]$; with the integral (effective) viscosity of the melt being able to rise by an order of magnitude (up to about 60 times higher). The newly-created mathematical model was verified by real orbital and ground crystallization processes for GaSb:In using the Bridgman method. The model approximations are shown to be adequate to the key hydrodynamic processes taking place in the melt and accompanying melt crystallization under various gravity conditions [9].

In these studies the particular attention was given to A_3B_5 compounds crystallization from unstoichiometric melts-solutions based on their own low-melting point component A_3 (A_3 = Ga, In), such crystallization methods being widely used in the epitaxy growth processes. The main distinguishing feature of such crystallization systems is a very steep slope of the liquidus curve on the T-X phase diagram which is indicative of large equilibrium crystallization temperature dependence on B_5 concentration in the melt. For instance, dT/dX in the In-InP system reaches 25–30 K/at.%. B_5 (B_5 = P, As, Sb) is the crystal forming component, but its concentration in the liquid phase is relatively low (normally about 10–20 atom percent). Its behaviour in the process of crystal growth is analogous to that of impurities with distribution coefficient $k > 1$, at the interface it creates a depleted intermediate layer of melt-solution with lower equilibrium crystallization temperature. Since the transient layer thickness and concentration profile are to a large extent dependent on the intensity of diffusion and/or convective transfer within the liquid zone, the processes of crystallizing A_3B_5 compounds from the melt-solution are extremely gravity-sensitive [10]. Besides impurity inhomogeneity (if a doped melt was used) this sensitivity also manifests itself on the level of crystal structural perfection.

A detailed study has been carried out of reference- and space-grown single crystals of InP:S processed by the low-temperature (1143 K) traveling heater method from a melt whose initial equilibrium composition was 84 at.% of indium, 16 at.% of phosphorus and $2.2 \cdot 10^{18}$ at/cm^3 of sulphur onboard "Foton-11" space vehicle under the Russian-German SKAT-FD programme (see [11]). Quality assessment of the crystals so grown with regard to homogeneity of their properties (dopant distribution) and crystallographic perfection was performed based on the results of a set of complementary studies.

A comparison of crystallization mechanisms in crystals' own stoichiometric melts and unstoichiometric melts showed that the latter differ essentially in that they require taking into account the effects of transient (interfacial) layer constitutional undercooling in a situation where convection is reduced so drastically even if the growth rates are very low [12]. The consequences of a developing diffusion mode are the *delta*-layer depleted in phosphorus and unsteady; early development of a cellular substructure in crystals; phase structuring of the transient layer with forming clusters observed in space-grown crystals (Fig. 2b). The reference ground sample did not have such inclusions. It is shown that the defects are spherical ordered micro-precipitates of the second phase based on the solvent (In), maximally concentrated in the (111) plane, they are 10–

20 micrometers in diameter and their density in the crystallized layer cross-section is ~$4 \cdot 10^4$ cm^{-2}. A hypothesis was put forward and formulated mathematically on the clusters formation in stagnant melt-solution near the crystallization front under zero gravity and excessive oversaturation in In conditions with the clusters' subsequent incorporation into the growing InP crystal. The following values were determined experimentally: sulphur impurity distribution coefficients $k_0 = 0.274$ and $k_{eff.} = 0.430$, the coefficient of sulphur atoms diffusion in the melt-solution $D(S) = 4.2 \cdot 10^{-7}$ cm^2/s, as well as the effective thickness of the transition layer *delta* = 0.07 cm under normal terrestrial gravity conditions.

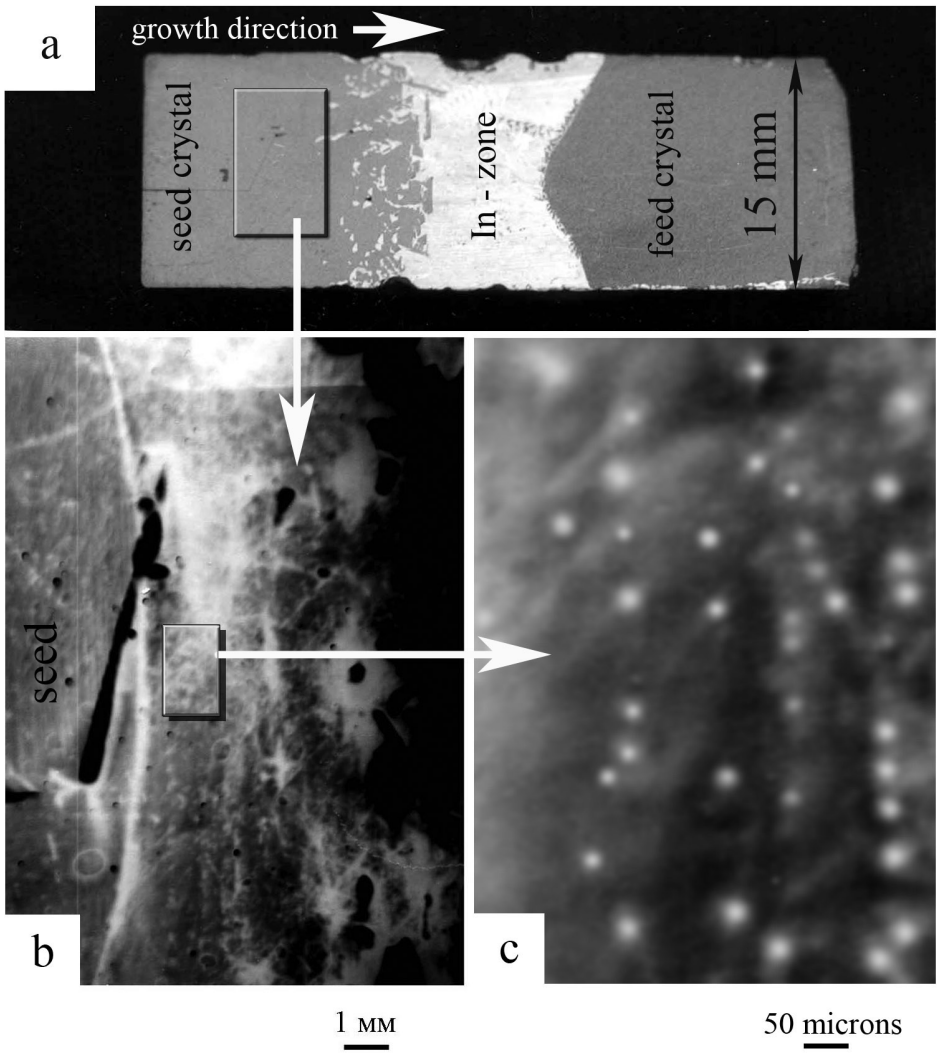

Fig. 2. a — view of the longitudinal axial section of InP sample after 50 hours of growing a single crystal layer by the traveling heater method in space; b — X-ray topography of the grown layer, general view; c — parallel chains of "giant" spherical microdefects, revealed near the seeding front by high resolution X-ray scanning topography. See Refs [12, 13] in detail

The data obtained are used as benchmarks in the generalized model now being developed of crystallization processes under zero gravity. To take into account the finite interval of temperature undercooling (ΔT) in real "space" InP:S crystallization processes additional linear dependence of enthalpy on the temperature in the undercooling region, and density thermal dependence for the

material in the melt transition layer at the interface containing clusters were introduced for the first time. By that a high degree of adequacy was achieved in the model approximations of experimentally revealed peculiarities of A_3B_5 single crystal growth from crystals' own non-stoichiometric melt-solutions. Calculations have shown that In-microdefects can arise in the special case that the melt-solution in the area near the crystallization front is locally depleted in phosphorus down to its zero concentration. Our estimates show that this situation corresponds to the constitutional undercooling depth ΔT of about 4K or more [13].

Conclusion

So, the use of microgravity is validated for the study of structural self-organization processes (cluster forming) in melts during their solidification; early positive results have been obtained. The investigations along this new line of inquiry in microgravity physics continue in 2006-2008 under support of RFBR Grant #06-02-16597 "*The fine structure of transient layer and microkinetics of interface building in processes of microgravity semiconductors single crystal melt growth*".

The opportunity to carry out fundamental model generalizations and test the proposed approaches will be used in the study of dendrite crystallization of intermetallic compounds TiAlNb within the framework of *IMPRESS* project, with there being a potential of performing crystallization experiments on both orbital (*ISS*, the *Destiny* module), and suborbital (*MAXUS*, *TEXUS*) microgravitation platforms in 2007–2009.